

Proton Diffusion and T_1 Relaxation in Polyacrylamide Gels: A Unified Approach Using Volume Averaging

Brigita Penke,^{*1} Stephen Kinsey,^{†2} Stephen J. Gibbs,^{*†} Timothy S. Moerland,^{†‡} and Bruce R. Locke^{*†3}

^{*}Department of Chemical Engineering, FAMU-FSU College of Engineering, 2525 Pottsdamer Street, Tallahassee, Florida 32310-6046;

[†]Center for Interdisciplinary Magnetic Resonance, National High Magnetic Field Laboratory, Tallahassee, Florida;

and [‡]Department of Biological Sciences, Florida State University, Tallahassee, Florida

Received January 13, 1998

The structure of polyacrylamide gels was studied using proton spin-lattice relaxation and PFG diffusion methods. Polyacrylamide gels, with total polymer concentrations ranging from 0.25 to 0.35 g/ml and crosslinker concentrations from 0 to 10% by weight, were studied. The data showed no effect of the crosslinker concentration on the diffusion of water molecules. The Ogston-Morris and Mackie-Meares models fit the general trends observed for water diffusion in gels. The diffusion coefficients from the volume averaging method also fit the data, and this theory was able to account for the effects of water-gel interactions that are not accounted for in the other two theories. The averaging theory also did not require the physically unrealistic assumption, required in the other two theories, that the acrylamide fibers are of similar size to water molecules. Contrary to the diffusion data, T_1 relaxation measurements showed a significant effect of crosslinker concentration on the relaxation of water in gels. The model developed using the Bloch equations and the volume averaging method described the effects of water adsorption on the gel medium on both the diffusion coefficients and the relaxation measurements. In the proposed model the gel medium was assumed to consist of three phases (i.e., bulk water, uncrosslinked acrylamide fibers, and a bisacrylamide crosslinker phase). The effects of the crosslinker concentration were accounted for by introducing the proton partition coefficient, K^{eq} , between the bulk water and crosslinker phase. The derived relaxation equations were successful in fitting the experimental data. The partition coefficient, K^{eq} , decreased significantly as the crosslinker concentration increased from 5 to 10% by weight. This trend is consistent with the idea that bisacrylamide tends to form hydrophobic regions with increasing crosslinker concentration. © 1998 Academic Press

Key Words: polyacrylamide gels; PFGNMR; water self-diffusion; T_1 relaxation.

INTRODUCTION

A detailed understanding of the structure of hydrogels and the dynamics of molecular motion of solutes in hydrogels is important for a number of applications in biochemical separation, including gel permeation chromatography and gel electrophoresis, and for biomedical drug delivery processes that use hydrogels as carriers. In addition, hydrogels have potential as experimental models of biological tissue. Hydrogel structures in general have been analyzed by a number of methods including dynamic light scattering (1–3), electron microscopy, laser light scattering (4), small angle X-ray scattering (3, 5), osmotic swelling (6–8), atomic force microscopy (9), NMR imaging (10), NMR T_1 and T_2 relaxation methods (11–14), and magnetization transfer methods (15–17). Despite the wide range and number of these studies, there remain some very important unresolved issues concerning the structure of these gels and the relationships between gel structure and diffusive transport within the gel.

One of the most extensively used and studied hydrogels is polyacrylamide. Polyacrylamide gels are synthesized by chemical or photochemical crosslinking of the bifunctional crosslinking agent, bisacrylamide, with the acrylamide monomer. The structure of crosslinked hydrogels has been interpreted within the context of a random network of fibers following the early work of Ogston (18). Ogston's original analysis has been applied and extended extensively within the gel electrophoresis and gel chromatography literature (19–23). Gel structure also has been interpreted within a broader range of structures to include distributions of variously shaped pores (24, 25). Richards and Temple (26) applied and extended the Ogston theory to the analysis of the structure of crosslinked polyacrylamide gels in order to account for the effects of crosslinker concentration on the microscopic structure of the gel. They interpreted results on osmotic swelling and gel permeation chromatography within the context of deviations from an ideal gel where all functional ends of the monomers and crosslinkers are fully reacted. Deviations from the ideal gel lead to clustering and clumping of microscopic regions of the

¹ Present address: Merck & Co., Inc., Flint River Plant, 3517 Radium Springs Road, Albany, GA 31705.

² Present address: Department of Biological Sciences, University of North Carolina at Wilmington, Wilmington, NC.

³ To whom correspondence should be addressed. Fax: (850) 487-6150. E-mail: locke@eng.fsu.edu.

less water-soluble bisacrylamide. Further support for the existence of microscopic (i.e., on the nanometer length scale) heterogeneities within polyacrylamide gels has been provided by light scattering studies (3, 5, 6). These studies indicate the existence of heterogeneous domains whose sizes vary with the amount of crosslinker. As the crosslinker concentration increases, the scattering results have been interpreted as either the development of increasingly thicker fiber strands of acrylamide (5) or as increasing-diameter globular regions of less water-soluble bisacrylamide (3). The exact nature of these structures and the effects of crosslinker concentration on these structures have not been fully confirmed.

Diffusive transport of large and small solutes in hydrogels has been studied by gel permeation chromatography (27–29), diffusion cells (30), light scattering (31, 32, 33), pulsed field gradient NMR (34–37), and other methods (38). Diffusion of solutes in hydrogels is expected to depend upon the size of the probe relative to the size of the pore spaces in the gel, the geometry of the gel structure, and various physical/chemical interactions between the probe species and the gel matrix. In order to account for probe size, the Ogston theory has been extended to diffusion (and electrophoresis) (27, 28, 39) whereby the partition coefficient has been equated to the ratio of the diffusion coefficient in the gel to that in free solution. Other approaches, including hindered transport theory (40, 41), have also been used to describe the effects of solute size on diffusion. Experimental data typically has been interpreted on the basis of a stretched exponential equation (36, 42–44) which can be justified theoretically through comparison with Monte Carlo simulations or derived using a specific arrangement of a unit cell. Despite these studies, a full range of experimental measurements on probe diffusion in polyacrylamide gels as functions of gel composition, including crosslinker density, has not been reported; in addition, the effects of media geometry and solute–gel interactions have not been incorporated within one comprehensive approach.

In order to account for the effects of media geometry and gel interactions of small solutes diffusing in porous structures, the method of volume averaging pioneered by Whitaker (45, 46) can be used. The volume averaging approach also has been applied to transport in porous media where the solute has adsorptive interactions with the matrix (47–49). While adsorption effects may be expected to play a major role on diffusion in gels, current theory indicates that diffusion in isotropic media may be less sensitive to the exact arrangement of the physical elements of the media (50, 51).

The present study seeks to address the specific effects of probe interaction with the gel and gel structure on the diffusion of water by applying the method of volume averaging to the analysis of proton T_1 relaxation and PFG water self-diffusion data in polyacrylamide gels with various acrylamide and crosslinker concentrations. A detailed model of the polyacrylamide structure is proposed whereby the gel contains three regions: the acrylamide fibers, regions of concentrated bisac-

rylamide, and bulk water. The method of volume averaging is applied to the Bloch equations (52) for the bulk magnetization in the three domains. Transport in the bulk fluid and adsorption of water to the acrylamide fibers and bisacrylamide domains are included in the Bloch model, following the work of Cohen and Mendelson (53–55). The averaging process leads to expressions for the effective diffusion and relaxation coefficients as functions of the specific solute–gel interaction parameters and the geometry of the gel matrix. The water self-diffusion data obtained by NMR is compared to the above mentioned theory as well as to several other theories found in the literature, and T_1 relaxation data are interpreted in the context of volume averaging theory.

MATERIALS AND METHODS

Gel Preparation

Polyacrylamide hydrogels were synthesized by copolymerization of acrylamide with the tetrafunctional crosslinking agent, *N,N'*-methylenebisacrylamide (Bis) by redox reaction, using the reagents ammonium persulfate (APS) and tetramethylethylenediamine (TEMED). Gels were prepared from concentrated (30 or 40% (wt of polymer/100 ml)) stock solutions of acrylamide and crosslinker (%T) (Bio-Rad) and appropriate amounts of 500 mM tris(hydroxymethylaminomethane) (Tris) buffer solution and deionized water. Buffer solution was prepared by dissolving tris(hydroxymethylaminomethane) (Bio-Rad) in deionized water and adding 6 N HCl to obtain pH 6.8. The final concentration of buffer solution in the gels was 125 mM Tris.

For PFG diffusion measurements, the concentration of the monomer was varied between 2.5 to 35 (%T) (weight of acrylamide + Bis/100 ml solution). For spin–lattice relaxation measurements, the concentration of monomer was varied between 2.5 and 20 %T. The crosslinker concentration was varied between 0 and 10 %C (weight percent of crosslinker/weight of acrylamide + bisacrylamide). Sample solutions were brought to and maintained at room temperature (23°C) by water bath incubation for 20 min prior to and during a 15-min vacuum degassing. The reagents APS (0.1 g/ml) and TEMED were added in microliter amounts immediately after the degassing. All reagents were analytical grade and purchased from Bio-Rad (Hercules, CA).

For PFG diffusion measurements gels were cast in micropipette capillary tubes (#21-164-2H, Fisher Scientific, Pittsburgh, PA). For spin–lattice relaxation measurements, gels were cast in Wilmad Glass (Buena, NJ) 5.0-mm-diameter NMR tubes. Gelation in both the capillary and 5.0-mm tubes occurred within 30 min at room temperature (23°C). Gels were left overnight before any NMR measurements and were stored at 4°C under high humidity. Gels used in this study were not washed or soaked in water prior to the measurements. Thus, they are considered to be incompletely swollen gels.

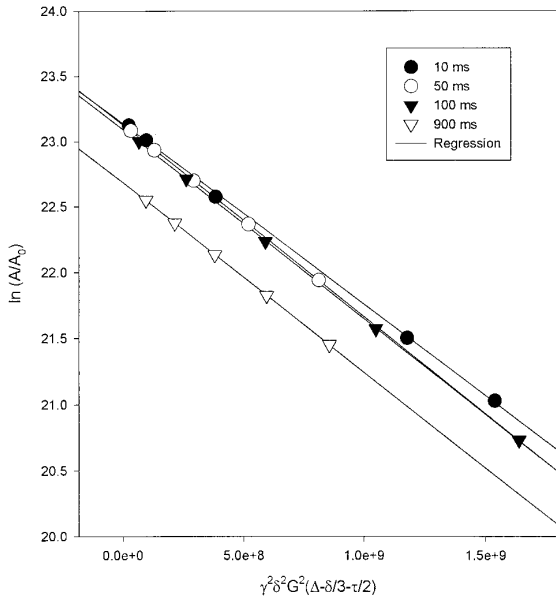


FIG. 1. Normalized echo intensity as a function of the gradient strength at $\Delta = 10, 50, 100, 900$ ms.

Determination of Diffusion Coefficients Using PFG NMR

Diffusion of water molecules in polyacrylamide gels and solutions were studied using a 600-MHz Bruker DMX spectrometer coupled with a 14-T 89 mm-bore Bruker/Magnex magnet. The experiments were conducted at ambient temperature (approximately 25°C). The diffusion measurements were performed using the bipolar pulse pair (BPP) longitudinal eddy-current delay (LED) stimulated-echo sequence (56–58) which effectively eliminates the effects of eddy currents and sample-induced background gradients. Diffusion coefficients were obtained using (59)

$$y(\delta G, \Delta) = \ln \frac{A(G)}{A(0)} = -\gamma^2 \delta^2 G^2 D (\Delta - \delta/3 - \tau/2), \quad [1]$$

where $A(g)$ and $A(0)$ are the echo intensity in the presence and absence of the gradients respectively, G is the gradient strength, $\delta/2$ is the duration of the gradient pulse, D is the diffusion coefficient, τ is the time interval between the successive pulses, and Δ is the time interval between the successive gradient pairs. The measurements were performed by varying the gradient strength G . The gradient pulse duration δ was 2 ms, and the time intervals Δ equal to 10, 50, 100, and 900 ms were used with each gradient strength G . Representative data are shown in Fig. 1, which depicts the logarithm of normalized magnetization intensity as a function of $\gamma^2 \delta^2 G^2 (\Delta - \delta/3 - \tau/2)$ for 20% T/5% C gel with Δ equal to 10, 50, 100, and 900 ms.

Spin–Lattice Relaxation Measurements

^1H spin–lattice relaxation measurements were performed on a Bruker 270-MHz spectrometer coupled with a 7.05-T (charged to 6.3 T) 89-mm-bore Bruker magnet. Experiments were conducted at 28°C. T_1 relaxation measurements were obtained using the inversion-recovery pulse sequence. All measurements were obtained using eight scans with an intervening 15-s delay. A total of 30–40 data points were collected as a function of recovery time t , which was varied between 0.001 and 13 s, and in general the increments were not equally spaced.

Spin–lattice relaxation measurements were also obtained for 125 mM Tris buffer solution, which is the final concentration of buffer in gels. The relaxation time, T_1 , for buffer solution only was obtained using a three-parameter fit to the equation

$$\frac{M}{M_0} = \left[1 - k \exp\left(-\frac{t}{T_1}\right) \right], \quad [2]$$

where k is ideally equal to 2. Fitting the data for 125 mM Tris solution to Eq. [2], k was equal to 1.89 and T_1 was equal to 3.97 s.

DERIVATION OF MAGNETIZATION RECOVERY EQUATIONS FOR PROTON RELAXATION IN GEL MEDIA

Polyacrylamide gel is considered in the present study as a three-phase porous medium, consisting of uncrosslinked polyacrylamide fibers, semipermeable clusters of the bisacrylamide crosslinker, and free water in the void phase between the other regions (Fig. 2). This model is based upon previously published experimental and theoretical results (3, 5, 26) that indicate that the crosslinker can form a separate, less water-soluble phase.

The proton magnetization M_b , M_f , and M_β within the bulk water volume, on the surface of the fibers, and in the clusters of crosslinker, respectively, are described using the Bloch equations (52). The proton magnetization is directly proportional to the spin densities N_b , N_f , and N_β in the bulk fluid, on the surface of the fibers, and in the clusters of crosslinker, respectively. The decay of proton magnetization occurs as a result of spin relaxation in the bulk liquid phase, in the clusters of crosslinker, and at the surface of the fibers, and is also due to the diffusion in the bulk and in the crosslinker phases. As shown in Fig. 2, the gel medium consists of two main phases: the α phase, which is composed of bulk water and the acrylamide fibers, and the β phase, which consists of clusters of crosslinker. In order to solve for the effective relaxation constant in this medium, the volume averaging method developed by Whitaker and co-workers (46, 50, 60–62) was applied to the Bloch equations (52). This methodology allows for convenient and rapid estimation of the effects of structure and

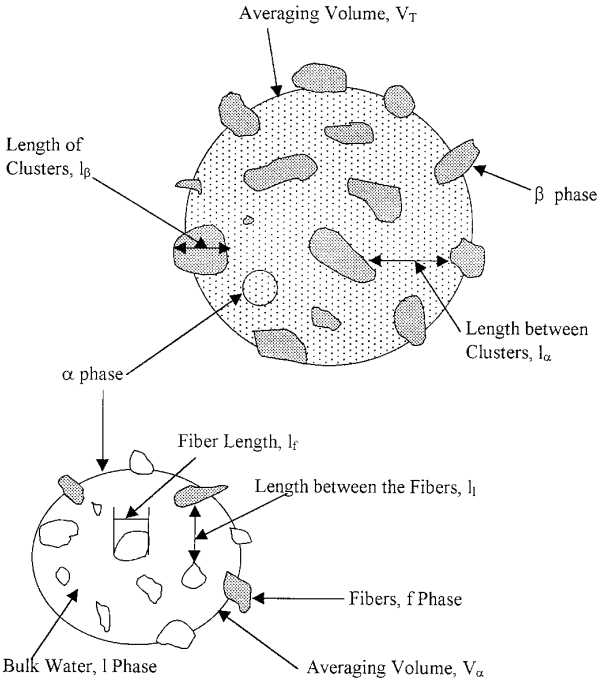


FIG. 2. Gel medium model, composed of bulk water and fiber, α , phase, and crosslinker cluster phase, β .

water-gel interactions on the observable properties of the medium including the diffusion and effective relaxation parameters. The α phase (Fig. 2) is subdivided into two “microphases” consisting of uncrosslinked fibers of polyacrylamide, f , and bulk water, l . The appropriate Bloch equations (52) for this phase are

$$\frac{\partial M_l}{\partial t} = D_l \nabla^2 M_l - \frac{(M_l - M_l^\infty)}{T_{1l}} \quad \text{in } V_l \quad [3]$$

$$-n_{lf} \cdot D_l \nabla M_l = \sigma(PM_l - M_f) \quad \text{at } A_{lf} \quad [4]$$

$$\begin{aligned} \frac{\partial M_f}{\partial t} &= D_f \nabla^2 M_f - \frac{(M_f - M_f^\infty)}{T_{1f}} \\ &+ \sigma(PM_l - M_f) \quad \text{at } A_{lf}. \end{aligned} \quad [5]$$

Cohen and Mendelson (53) considered a similar problem; however, their approach did not utilize the volume averaging method to derive the effective transport and relaxation parameters and they did not include the α phase equation in combination with the magnetization equations for the crosslinker phase, β , introduced later. In Eqs. [3]–[5], D_l and D_f are the diffusion coefficients of protons in the bulk fluid and on the surface of the fibers, respectively. T_{1l}^{-1} and T_{1f}^{-1} are the bulk and surface relaxation times, σ is the detachment rate per proton of protons on the surface of the fibers, and P is the adsorption coefficient to the surface of the fibers, $M_f^{\text{eq}}/M_l^{\text{eq}}$. M_l^∞ and M_f^∞ are the asymptotic magnetization values of the protons

in the bulk water and on the surface of the fibers, and n_{lf} is the unit normal directed away from the surface. In Eq. [5] the first term on the right-hand side is the surface diffusion term, the second reflects the relaxation on the surface of the fibers, and the third term reflects the proton transfer rate from the surface of the fibers to the bulk fluid. Cohen and Mendelson (53) have previously shown using order of magnitude estimates that the fiber surface diffusion term $D_f \nabla^2 M_l$ is small in comparison to the rest of the terms in Eq. [5], and can be neglected.

In order to obtain a one-equation model for the entire system, the above equations must be volume averaged in the α phase (Fig. 2) and then combined with the averaged equations in the β phase (Fig. 2). For the β phase, consisting of crosslinker clusters, the governing equation contains the diffusion and relaxation terms

$$\frac{\partial M_\beta}{\partial t} = D_\beta \nabla M_\beta - \frac{(M_\beta - M_\beta^\infty)}{T_{1\beta}} \quad \text{in } V_\beta, \quad [6]$$

where D_β is the proton diffusion coefficient in the crosslinker phase, $T_{1\beta}$ is the relaxation time (s), and M_β^∞ is the asymptotic magnetization. At the interface between the two phases, the diffusion fluxes are equal as given by

$$-n_{\beta\alpha} \cdot D_\beta \nabla M_\beta = -n_{\beta\alpha} \cdot D_{\text{eff}}^\alpha \nabla M_\alpha \quad \text{at } A_{\alpha\beta}, \quad [7]$$

where $n_{\beta\alpha}$ is the unit normal directed from the β phase into the α phase. D_{eff}^α is the effective diffusion coefficient in the α phase, and M_α is the magnetization in the α phase, obtained by volume averaging the magnetization over the f and l phases. Since the β phase is assumed to be permeable, at the interface between the two phases the magnetization density difference between the α and β phases is equal to the diffusive flux from the β phase

$$-n_{\beta\alpha} \cdot D_\beta \nabla M_\beta = B(M_\beta - K^{\text{eq}} M_\alpha) \quad \text{at } A_{\alpha\beta}, \quad [8]$$

where B is the rate coefficient for transfer into the β phase, and K^{eq} is the equilibrium distribution coefficient into the β phase. When the governing equations for the β phase are combined with the averaged equation for the α phase, the problem becomes similar to that developed by Ochoa *et al.* (63) for cellular media with reaction and diffusion in two phases.

In order to relate magnetization in the l and f phases to the magnetization density of the entire sample, which is the measured quantity, the first step requires obtaining the average magnetization in the α phase. For any point in the f and l phases, there is an associated averaging volume, V_α . The phase average quantities are obtained by averaging the governing equations. For the l phase, one has

$$\begin{aligned} & \frac{1}{V_\alpha} \int_{V_l} \frac{\partial M_l}{\partial t} dV \\ &= \frac{1}{V_\alpha} \int_{V_l} D_l \nabla^2 M_l dV - \frac{1}{V_\alpha} \int_{V_l} \frac{(M_l - M_l^\infty)}{T_{1l}} dV \text{ in } V_l. \end{aligned} \quad [9]$$

The length scales associated with the averaging volume are discussed in detail by Carbonell and Whitaker (46). The main requirement is that the radius of the averaging volume be large in comparison to the lengths of l_l and l_f , and small in comparison to the length scale, L_α , over which significant changes in the average quantities occur:

$$l_l \ll r_0 \ll L_\alpha \quad [10]$$

$$l_f \ll r_0 \ll L_\alpha \quad [11]$$

Since the spin–lattice relaxation measurements are obtained using various time delays (0.001–12 s) between the RF pulses, the r_0 value, using $r_0 = (2Dt_{\text{delay}})^{1/2}$, ranged from 2 to 230 μm . The half-length of the RF coil, L_α , surrounding the sample was 0.5 cm. The length of the fibers, l_f , is of order of 1 nm (64). Since the maximum crosslinker concentration was 10% C, the space between the fibers, l_l , is not expected to exceed 50 nm (65). Thus, the constraints given by Eqs. [10] and [11] are fully satisfied in the present study. It is very important to note that the length scales for the averaging volume are on the micron scale and thus information on the nanometer length scale cannot be directly determined from this type of measurement.

The phase average magnetization density in the l phase is defined as

$$\langle M_l \rangle = \frac{1}{V_\alpha} \int_{V_l} M_l dV \text{ in } V_l. \quad [12]$$

The phase averages are defined similarly at the surface of the fibers. The phase averaged governing magnetization equation in the l phase becomes

$$\frac{\partial \langle M_l \rangle}{\partial t} = D_l \langle \nabla^2 M_l \rangle - k_l \langle M_l - M_l^\infty \rangle \text{ in } V_l. \quad [13]$$

Here, the bulk fluid relaxation time, T_{1l} , is replaced by the reciprocal of k_l , the relaxation rate constant, and subscript l is dropped from this point on for convenience. The relaxation rate constant k_l and the diffusion coefficient D_l are assumed to have negligible variations in the l phase.

By applying the volume averaging theorem (45, 66) to the governing magnetization equation in the l phase, the equation

$$\begin{aligned} & \epsilon_l \frac{\partial \langle M_l \rangle^l}{\partial t} \\ &= D_l \nabla \cdot \left\{ \nabla (\epsilon_l \langle M_l \rangle^l) + \frac{1}{V_\alpha} \int_{A_{lf}} \underline{n}_{lf} M_l dA \right\} \\ &+ D_l \frac{1}{V_\alpha} \int_{A_{lf}} \underline{n}_{lf} \cdot \nabla M_l dA - k_l (\epsilon_l \langle M_l \rangle^l - M_l^\infty) \text{ in } V_l \end{aligned} \quad [14]$$

results, where the phase average magnetization density $\langle M_l \rangle$ is replaced with the intrinsic average quantity, $\langle M_l \rangle^l$:

$$\langle M_l \rangle = \epsilon_l \langle M_l \rangle^l \text{ in } V_l. \quad [15]$$

Here ϵ_l is the volume fraction of the bulk liquid phase, defined as

$$\epsilon_l = \frac{V_l}{V_\alpha}. \quad [16]$$

The asymptotic value M_l^∞ is a constant and does not change within the averaging volume.

By following the solution methodology outlined by Ochoa *et al.* (63), the one-equation model for the α phase can be shown to be given by

$$\begin{aligned} & (\epsilon_l + P - \epsilon_l P) \frac{\partial M_\alpha}{\partial t} \\ &= D_l \nabla \cdot \left\{ \epsilon_l \nabla M_\alpha + \frac{\epsilon_l}{V_l} \int_{A_{lf}} \underline{n}_{lf} \tilde{M}_l dA \right\} \\ &- (k_f P (1 - \epsilon_l) + k_l \epsilon_l) M_\alpha + \left(\frac{A}{V_\alpha} \right) k_f (M_f^\infty) + k_l (M_l^\infty), \end{aligned} \quad [17]$$

where \tilde{M}_l is the spatial deviation term, $\{\tilde{M}_l = M_\alpha - \langle M_l \rangle^l\}$. The surface relaxation time T_{1f} is replaced by the reciprocal of k_f , the relaxation rate constant, and M_α is the equilibrium weighted spatial average magnetization in the α phase, given by

$$M_\alpha = \epsilon_l \langle M_l \rangle^l + \frac{1}{P} \langle M_f^\infty \rangle \text{ in } V_\alpha. \quad [18]$$

Equations similar to that of Eq. [18] have been obtained for local mass equilibrium by Whitaker (47) for a multiphase diffusion and reaction problem or for local thermal equilibrium (67) in multiphase conduction problems. Here $\langle M_f^\infty \rangle$ is the magnetization density at the surface of the fibers. The surface

relaxation rate constant, k_f , proton detachment rate, σ , and equilibrium coefficient, P , are assumed to have negligible variations at the interface, A_{β} . In addition, the intrinsic average magnetization, $\langle M_l \rangle^l$, is assumed to be a constant at the interface. This assumption was investigated previously (46) and shown to be a valid approximation, provided

$$\left(\frac{r_0}{L_\alpha}\right)^2 \ll 1. \quad [19]$$

For the system studied, this constraint is easily satisfied: Since the maximum r_0 value is 250 μm , and L_α is 0.5 cm, the ratio $(r_0/L_\alpha)^2 = 0.002 \ll 1$.

Analogous to the development of Nozad *et al.* (60), one can define a closure problem for the local deviation term, \tilde{M}_α , and express the governing equation for the α phase in terms of the effective diffusion and reaction terms

$$\begin{aligned} \frac{\partial M_\alpha}{\partial t} &= \underline{D}_{\text{eff}}^\alpha : \nabla \nabla M_\alpha - k_{\text{eff}}^\alpha M_\alpha \\ &+ \frac{\left(\frac{A}{V_\alpha}\right) k_f (M_f^\infty) + k_l (M_l^\infty)}{P(A/V_\alpha) + \epsilon_l (1 - P(A/V_\alpha))}, \end{aligned} \quad [20]$$

where the effective diffusivity and relaxation rate constants are defined by

$$\frac{\underline{D}_{\text{eff}}^\alpha}{D_l} = \frac{\epsilon_l}{\epsilon_l (1 - P(A/V_\alpha)) + P(A/V_\alpha)} \left(\underline{I} + \frac{1}{V_l} \int_{A_{\beta}} n_{\beta} \cdot \underline{f} dA \right) \quad [21]$$

$$k_{\text{eff}}^\alpha = \frac{P(A/V_\alpha) k_f + \epsilon_l (k_l - P(A/V_\alpha) k_f)}{P(A/V_\alpha) + \epsilon_l (1 - P(A/V_\alpha))}. \quad [22]$$

The expression for the vector function, \underline{f} , can be obtained by solving a closure problem similar to that of Nozad *et al.* (60). It must be noted that the porosity in the present system does not vary over the macroscopic domain since the polyacrylamide gel is uniform on this scale. In addition, since there is no diffusion in the fiber phase, f , the solution in the α phase is defined only by the closure problem in the l phase. The vector field, \underline{f} , is a function of σ , (PA/V_α) , and D_l . Whitaker (47) discusses in detail the constraints necessary to show under what conditions the closure problem is independent of the adsorption and relaxation processes. Furthermore, if the effects of cell geometry are ignored ($f \ll 1$), the diffusion coefficient is a function of the ratio (PA/V_α) and porosity, ϵ_l . It is interesting to note that the effective relaxation rate constant, k_{eff}^α , is not a function of geometry, and it is also not affected by the solution for the \underline{f} field. The effective relaxation rate constant, k_{eff}^α , varies with the porosity, ϵ_l , and is affected only by $P(A/V_\alpha)$, k_f , and k_l .

Volume Averaging in V_T and the One-Equation Model

The system of equations for the α and β phases (Eqs. [20], [6]–[8]) is similar to the problem solved by Ochoa *et al.* (63) involving diffusion and reaction in cellular media; however, the present system includes three relaxation terms and the adsorption factor, P .

Following the previously outlined methodology for the l and f phases, the governing equations for the α and β phases can be volume averaged in V_T (Fig. 2). As before, the magnetization density equations for the α and β phases are expressed in terms of the intrinsic phase average magnetization densities, $\langle M_\alpha \rangle^\alpha$ and $\langle M_\beta \rangle^\beta$. The resulting equations are combined into the one-equation model using the following expression:

$$\langle M \rangle = \epsilon_\alpha \langle M_\alpha \rangle^\alpha + \frac{1}{K^{eq}} \epsilon_\beta \langle M_\beta \rangle^\beta. \quad [23]$$

The governing one-equation model for the diffusion and relaxation rate constant in the porous medium becomes

$$\frac{\partial \langle M \rangle}{\partial t} = \underline{D}_{\text{eff}}^T : \nabla \nabla \langle M \rangle - k_{\text{eff}}^T (\langle M \rangle - M_{\text{eff}}^\infty), \quad [24]$$

where $\underline{D}_{\text{eff}}^T$ is defined as

$$\begin{aligned} \underline{D}_{\text{eff}}^T &= \frac{D_{\text{eff}}^\alpha}{(\epsilon_\alpha + K^{eq} \epsilon_\beta)} \left[(\epsilon_\alpha + \kappa \epsilon_\beta) \underline{I} + \frac{1}{V_T} \int_{A_{\alpha\beta}} \frac{1}{2} (n_{\alpha\beta} \underline{g} \right. \\ &\left. + \underline{g} n_{\alpha\beta}) dA + \frac{\kappa}{V_T} \int_{A_{\beta\alpha}} \frac{1}{2} (n_{\alpha\beta} \underline{h} + \underline{h} n_{\beta\alpha}) dA \right] \end{aligned} \quad [25]$$

and k_{eff}^T and M_{eff}^∞ are defined as

$$\begin{aligned} k_{\text{eff}}^T &= \frac{k_{\text{eff}}^\alpha \epsilon_\alpha + K^{eq} k_\beta \epsilon_\beta}{\epsilon_\alpha + K^{eq} \epsilon_\beta} \\ &= \frac{1}{\epsilon_\alpha + K^{eq} \epsilon_\beta} \left[\left(\frac{P(A/V_\alpha) k_f + \epsilon_l (k_l - P(A/V_\alpha) k_f)}{P(A/V_\alpha) + \epsilon_l (1 - P(A/V_\alpha))} \right) \epsilon_\alpha \right. \\ &\left. + K^{eq} k_\beta \epsilon_\beta \right] \end{aligned} \quad [26]$$

$$\begin{aligned} M_{\text{eff}}^\infty &= \frac{1}{k_{\text{eff}}^T (\epsilon_\alpha + K^{eq} \epsilon_\beta)} \\ &\times \left[k_\beta M_\beta^\infty + \frac{\left(\left(\frac{A}{V_\alpha} \right) k_f M_f^\infty + k_l M_l^\infty \right)}{P(A/V_\alpha) + \epsilon_l (1 - P(A/V_\alpha))} \right]. \end{aligned} \quad [27]$$

The vector fields, \underline{g} and \underline{h} , which are functions of the geometry of α and β phases, respectively, can be obtained by solving the

closure problem (60, 68). The vector field \underline{h} is also a function of the water partition coefficient into the β phase. In Eq. [25] κ is a function of D_β , the diffusion coefficient in the crosslinker phase, and K^{eq} , the permeability into the crosslinker phase:

$$\kappa = K^{eq} \frac{D_\beta}{D_{eff}^\alpha} \quad [28]$$

If the diffusion coefficient, D_β , in the crosslinker phase is small, or the permeability into the crosslinker phase is very low, the model predicts very little effect of crosslinker on the effective diffusivity. It must be noted that the proposed model assumes that the solute size is very small relative to structure of gel. In Eq. [26], ϵ_α and ϵ_β are the volume fractions of the α and β phases ($\epsilon_\alpha = V_\alpha/V_T$, $\epsilon_\beta = V_\beta/V_T$), and k_β or $(T_{l\beta})^{-1}$ is the relaxation rate constant in the crosslinker phase. In deriving Eq. [20], the length scale constraints

$$\frac{l_\alpha}{L} \ll 1 \quad [29]$$

$$\frac{l_\beta}{L} \ll 1 \quad [30]$$

were used, where L is the macroscopic length scale. For the present study, these constraints are easily satisfied, since l_α is no more than $1 \mu\text{m}$, l_β is on the length scale of 1 nm , and L is on the order of 1 cm .

It can be noted that the derivation in this paper leads to effective diffusion coefficients and relaxation parameters that resemble the ‘‘fast exchange’’ limits found in the literature whereby the proton exchange between the various ‘‘pools’’ is rapid. The present theory reduces to this limit when the closure problems for the effective transport parameters are in the quasi-steady limit and where it has been assumed that the adsorption and relaxation processes do not affect the closure. In the volume averaging approach, it is not necessary to make these assumptions (47), and further work can be proposed to more completely evaluate the terms in the closure methodology, especially for cases where time dependence of the diffusion coefficient is observed experimentally.

Equation [27] can now be solved over the macroscopic sample domain and compared to the experimental values obtained from the NMR experiments as shown in the following section.

Macroscopic Magnetization Equation Solution

In the previous section the spatially averaged magnetization equation (Eq. [24]) appropriate for a porous medium was obtained. Since the gels for the NMR measurements were cast in standard NMR test tubes, Eq. [24] is expressed here in cylindrical coordinates:

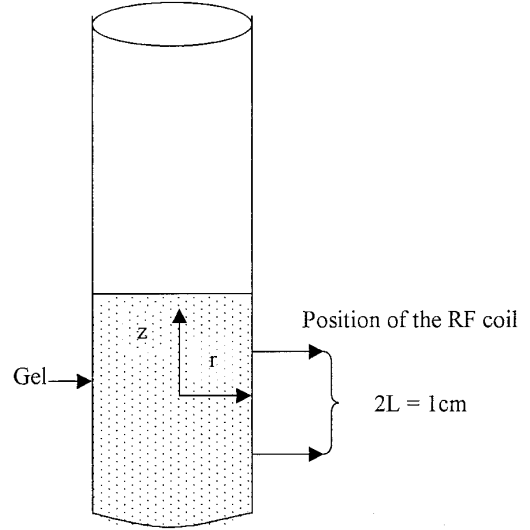


FIG. 3. The NMR tube with polyacrylamide gel.

$$\begin{aligned} \frac{\partial \langle M \rangle}{\partial t} = D_{eff}^T \left[\frac{1}{r} \frac{\partial}{\partial r} r \frac{\partial \langle M \rangle}{\partial r} + \frac{\partial^2 \langle M \rangle}{\partial z^2} \right] \\ - k_{eff}^T (\langle M \rangle - M_{eff}^\infty). \end{aligned} \quad [31]$$

It is assumed here that the diffusion medium is isotropic and the effective diffusivity does not vary spatially.

It is now desired to obtain the solution of this equation and to compare it to the experimental data. Figure 3 shows the NMR tube containing polyacrylamide gel and showing the position of the 1-cm RF coil on the outside of the tube. The coordinate axes are located at the center of the tube. Only those protons that are located in the area of the RF coil experience disturbances from the equilibrium magnetization condition. The no-flux condition is defined at the wall of the tube due to the impermeability and the zero-flux condition is defined at the center of the tube due to the symmetry

$$\frac{\partial \langle M \rangle}{\partial r} = 0 @ r = 0 \quad [32]$$

$$\frac{\partial \langle M \rangle}{\partial r} = 0 @ r = a \quad [33]$$

$$\frac{\partial \langle M \rangle}{\partial z} = 0 @ z = 0. \quad [34]$$

Since the proton magnetization is at its equilibrium on the outside of the RF coil, the boundary conditions at the ends of the tube are

$$\langle M \rangle = M_{eff}^\infty @ z = \pm L, \quad [35]$$

where L is the half-length of the RF coil. The initial condition for this problem is

$$\langle M \rangle = -M_{eff}^{\infty} @ t = 0. \quad [36]$$

In terms of normalized magnetization term averaged over both the r and z coordinates $\langle \langle M \rangle \rangle / M_{eff}^{\infty}$, the macroscopic solution to the system of equations (Eqs. [31]–[36]) is given by

$$\frac{\langle \langle M \rangle \rangle}{M_{eff}^{\infty}} = 1 - \left(\frac{16}{\pi^2} \right) \sum_{n=1}^{\infty} \frac{1}{(2n-1)^2} \times \exp(-k_{Teff}t) \exp\left(- \left[\frac{(2n-1)\pi}{2} \right]^2 D_{Teff}^T / L^2 \right). \quad [37]$$

For cases where the diffusion coefficient is very small, the magnetization is monoexponential as Eq. [37] would indicate when the exponential terms are dominated by the effective relaxation term, and in these cases Eq. [37] would reduce to Eq. [2] with k equal to 2, which is conventionally used for relaxation studies. It would be necessary for k_{eff}^T to be of order $(\pi/2)^2 D_{eff}^T / L^2$ for the additional terms in the series to be important. If k_{eff}^T were of order 0.3 s^{-1} , this would imply D_{eff}^T would need to be of order $10^{-2} \text{ cm}^2/\text{s}$ for the additional terms in the series to be needed. Provided D_{eff}^T is known, Eq. [37] can be used to determine the k_{eff}^T from the experimental data by fitting the magnetization recovery curve from the NMR mea-

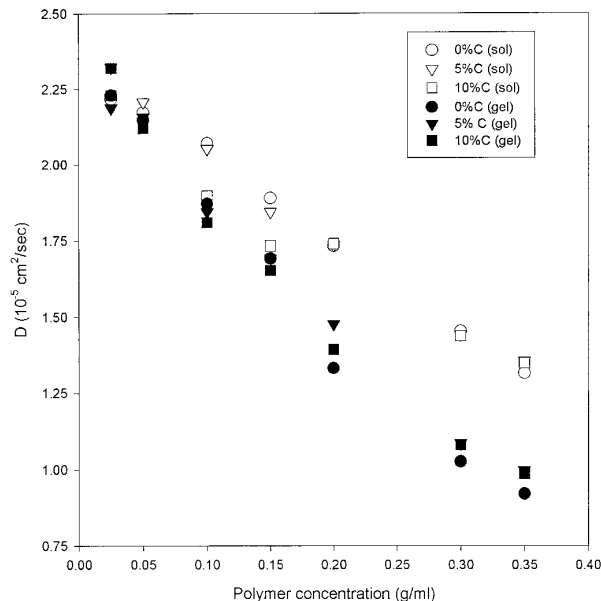


FIG. 5. Water diffusion in acrylamide solutions and polyacrylamide gels.

surements. In the present study, the values for the effective diffusion coefficient D_{eff}^T were determined by measuring the diffusion coefficients as described in the experimental section; however, for the present system the use of Eq. [37] leads to only a small correction over that obtained using Eq. [2] directly.

RESULTS

Diffusion

Diffusion coefficients were measured in gels and unpolymerized solutions with crosslinker concentration ranging from 0 to 10% C. The diffusion measurements were obtained at Δ ranging from 10 to 900 ms. No time dependence of the diffusion coefficients was observed within the examined Δ range. Figure 4 shows the diffusion coefficients from the present data and those reported by Pavesi and Rigamonti (34). For comparison, free water diffusion coefficients are also shown. Contrary to the results in the present study, Pavesi and Rigamonti (34) report time dependence of water diffusion coefficients in polyacrylamide gels at Δ times < 100 ms. Furthermore, the diffusion coefficients from Pavesi and Rigamonti (34) for polyacrylamide gels are much lower than those reported in the present study, which implies that the gels may have been prepared differently. The diffusion results can be affected by a large number of factors, such as hydrolysis, storage temperature, pH control, and time between the gel casting and NMR measurements.

In order to evaluate the effects of acrylamide and crosslinker concentration on water diffusion coefficients, the acrylamide content was varied between 2.5 and 30% T, and the crosslinker concentration was varied between 0 and 10% C. Diffusion coefficients at $\Delta = 900$ ms were chosen for this analysis.

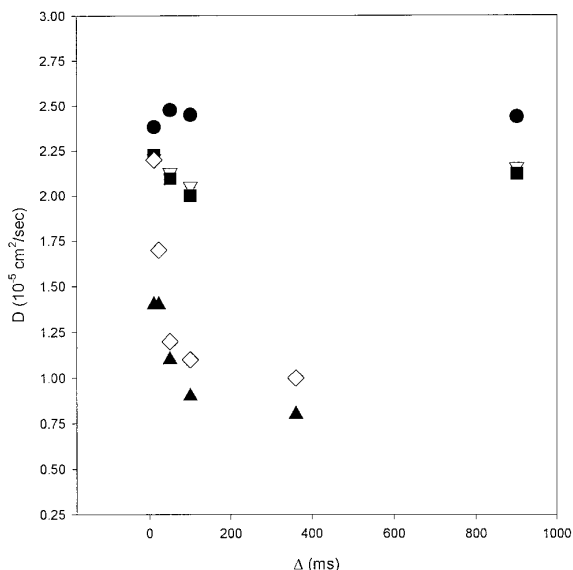


FIG. 4. Water self-diffusion in free water and polyacrylamide gels as a function of the diffusion time, Δ . Comparison to the Pavesi and Rigamonti (34) data. ●, in H_2O (present study); ▽, 5% T/5% C gels (present study); ■, 5% T/10% C gels (present study); ◇, 5% T/2.6% C gels (Pavesi–Rigamonti); ▲, 5% T/25% C gels (Pavesi–Rigamonti).

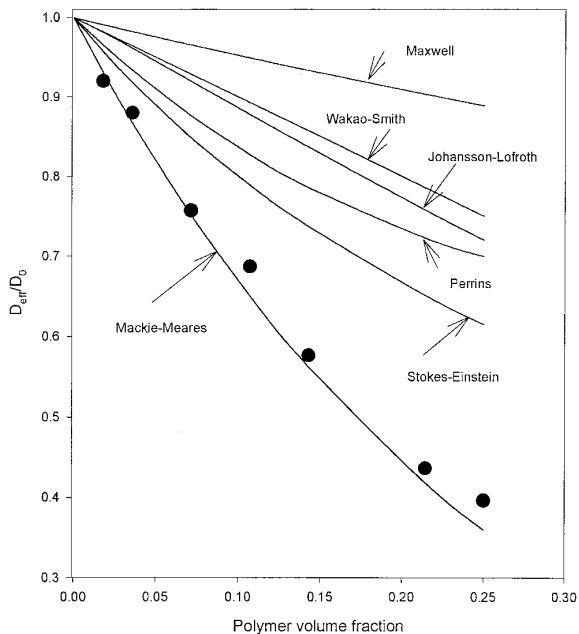


FIG. 6. Water diffusion in gels and comparison to the theoretical models.

Figure 5 shows the $D_{\text{H}_2\text{O}}$ in polyacrylamide gels and solutions with different crosslinker (0, 5, 10% C) concentrations. $D_{\text{H}_2\text{O}}$ in both solutions and gels decreases monotonically with increasing polymer concentration. At very low total acrylamide content (2.5–5% T), the diffusion coefficients in gels and solutions approach the free solution values, as expected. Neither gels nor solutions show any effect of crosslinker concentration on the diffusion coefficients of water. The diffusion coefficients for gels are lower than those for solutions, which indicates that the 3D network of gels formed upon polymerization changes the physical structure or the chemical properties of the local environment through which the water must diffuse.

In order to establish the structural (fiber size and shape) effects of gels on the diffusion of water, the experimental data was compared to various well-established models for fibrous media. For this analysis, the diffusion coefficients at $\Delta = 900$ ms were normalized with respect to the free water diffusion coefficient, $D_0 = 2.4 \times 10^{-5} \text{ cm}^2/\text{s}$ at $\Delta = 900$ ms. Since there was no significant difference between the diffusion coefficients at the same acrylamide and different crosslinker concentrations in gels and solutions, the diffusion values at 0, 5, and 10% C for each acrylamide concentration were averaged, normalized, and plotted against the volume fraction of polymer.

Figure 6 shows the measured normalized average diffusion coefficients for gels as a function of the polymer volume fraction. Also shown are the theoretical models developed by Maxwell (69), Perrins *et al.* (70) (this is numerically equivalent to the volume averaging result of Ryan (71)), Johansson-Lofroth (42), Wakao-Smith (72), Mackie-Meares (73), and Stokes-Einstein (74, 75). It can be noted that the theories of

Maxwell, Perrins *et al.*, Wakao and Smith, Mackie-Meares, and Stokes-Einstein do not contain any adjustable parameters. As a result, no fitting of these models to the data is required. The Johansson-Lofroth cell model (42), based upon the Ogston (18) expression for the probability distribution of straight polymer chains, requires knowledge of the fiber radius of the polymer. The Johansson-Lofroth model (42) was evaluated with a fiber radius of 5 Å (28). Other researchers have reported fiber radii as high as 6.5 Å (75) and as low as 3.5 Å (76), or observed the fiber radius to be dependent upon the crosslinker concentration (3, 5).

The Stokes-Einstein equation (74, 75)

$$\frac{D_{\text{eff}}}{D_0} = \frac{\eta_0}{\eta_{\text{eff}}} = (1 + 2.5\varphi)^{-1}, \quad [40]$$

where η_{eff} is the effective viscosity of the solution, and φ is the polymer volume fraction, predicted the diffusion coefficients in acrylamide solutions most accurately, as shown in Fig. 7. This expression was derived for diffusion of hard spheres in a dilute suspension moving in a continuum. The acrylamide solutions used in this study are relatively dilute, and the comparison indicates that the Stokes-Einstein equation (74, 75) is appropriate for these solutions. It is important to note that the Stokes-Einstein equation does not explicitly account for any specific molecular interactions between water and the acrylamide monomers; the increase in solution viscosity is sufficient to describe the reduction in diffusion coefficients.

As shown in Fig. 6, the Maxwell (69) model provides the upper limit for diffusion coefficients in isotropic two-phase media. The Perrins *et al.* (70) model, derived for a square

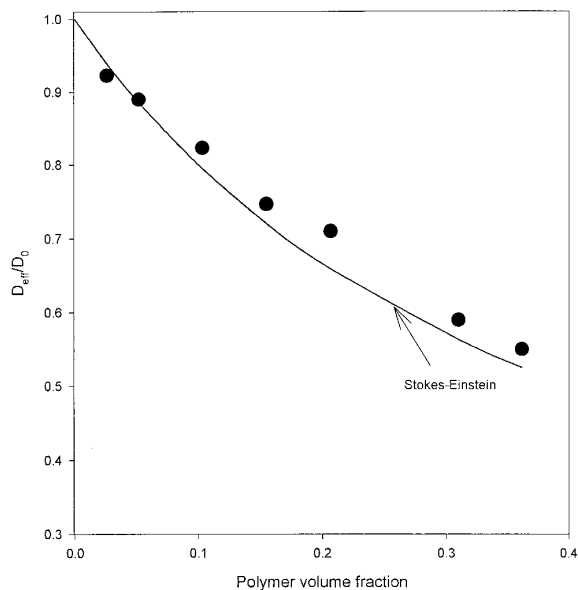


FIG. 7. Water diffusion in acrylamide solutions and Stokes-Einstein model.

lattice of cylindrical fibers, and the Johansson and Lofroth (42) model, derived for random suspension of cylindrical fibers, both predicted higher diffusion coefficients in gels than obtained experimentally (Fig. 6). The Perrins *et al.* (70) result is numerically similar to the calculations of Ryan (71) and Ochoa (49), who used volume averaging in arrays of squares and cylinders in a square lattice without including the adsorption terms. All three models predicted diffusion coefficients that were significantly higher than the experimental data. The major factors that may lead to the differences between the models and the data are adsorption effects and differences in geometry. Adsorption of water to the surface of the fibers will in general lower the diffusion coefficient. In addition, previous work (63) which explored the effects of geometry indicated that for isotropic media the effective diffusion coefficient is not highly dependent on the shape of the pores.

In addition, the Mackie and Meares (73) model,

$$\frac{D_{eff}}{D_0} = \left(\frac{1 - \varphi}{1 + \varphi} \right)^2 = \left(\frac{\epsilon}{2 + \epsilon} \right)^2, \quad [41]$$

matched the experimental data very closely, as shown in Fig. 6. This expression was originally developed for modeling diffusion in ion-exchange resin membranes. Mackie and Meares (73) used the lattice model for liquids where the resin polymer blocked a fraction φ of all sites available. The diffusion of solutes was then restricted to the free sites. In deriving this equation, Mackie and Meares (73) assumed that the obstacles, that is, lattice sites or polymer fibers in the present study, are of the same size as the solutes. Although, the polymer fiber size is expected to be larger (approximately 1-nm radius (65, 27)) than that of the water molecule (radius equal to 0.15 nm), the model predicted water diffusion coefficients in gels fairly well. Therefore, the major problems with using the Mackie–Meares theory are that it fails to account for adsorption effects and that the validity of the assumption concerning the relative size of fibers to solute size is questionable.

The experimental data in this study agree well with previously published results of Gibbs and Johnson (36) and Tokita *et al.* (78). Gibbs and Johnson (36) observed that their data for a wider range of solute sizes fit the Ogston–Morris (18, 39) model

$$f = \frac{D_{eff}}{D_0} = \exp\left(-\left(\frac{r_s + r_f}{r_f}\right)^2 Tv\right), \quad [42]$$

where f is the volume fraction available to the solute, r_s is solute radius (1.5 Å for water), r_f is the fiber radius, and v is the specific volume of the polymer. The comparison of the present study results to the Ogston–Morris (18, 39) model yielded r_f values equal to 1.5 Å for gels. The equivalent Stokes radius, which is the sum of the r_f and r_s , is equal to 3.0 Å. This value of r_f is much less than the values previously reported by Ogston

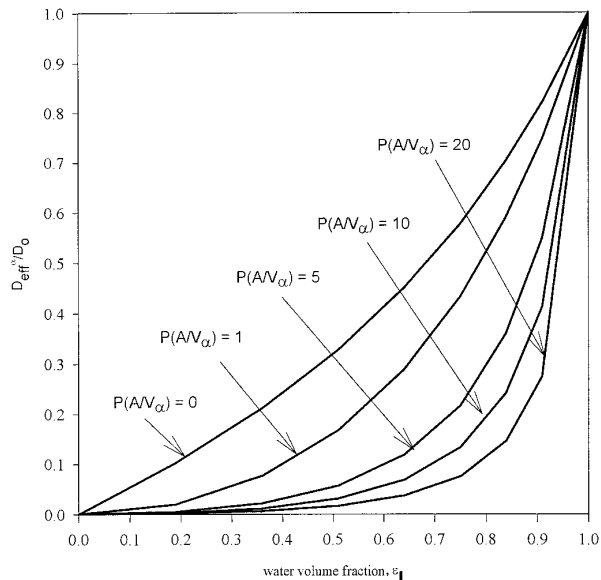


FIG. 8. Effects of the ratio $P(A/V_\alpha)$ on the effective diffusivities using the volume averaging model.

et al. (64), who used the sedimentation data of different size solutes in polyacrylamide solutions and Eq. [42] to obtain the fiber radii. They reported the radius of the polyacrylamide fiber as 9 Å in comparison to 1.5 Å found by fitting Eq. [42] to the results of the present study. A proposed radius size of 0.15 nm for the acrylamide fibers is rather small and may not reflect realistic features of the gel. In contrast to the present study of water diffusion, the previous research (65, 27) investigated the transport properties of much larger proteins (1.6–9 nm). It is therefore useful to consider other factors such as adsorption that may account for the decrease in the observed diffusion coefficients in gels. Furthermore, the model of Ogston–Morris (18, 39) does not provide any explanation for the lack of effect of crosslinker on the water diffusion in gels.

Contrary to the previously published models, the volume averaging model proposed in the previous section accounts for the effects of both adsorption and crosslinker concentration. Equation [21] demonstrates that when the adsorption coefficient, P , is increased, the diffusion coefficient will decrease, provided the ratio $P(A/V_\alpha)$ is not much less than 1. Figure 8 shows the effect of $P(A/V_\alpha)$ on the effective diffusivities in gels. The adsorption coefficient P is related to the water layer thickness at the surface of the fibers, which is expected to be on the order of 1 Å. The ratio of the fiber surface area to the total volume of the fiber and water in the α phase, A/V_α , is on the order of 1 nm^{-1} . As a result, the adsorption coefficient, P , can strongly affect the diffusion coefficients in gels. Furthermore, Eq. [25] demonstrates that the magnitude of the equilibrium coefficient for water in the crosslinker phase, K^{eq} , will directly affect the diffusion coefficients in crosslinked gels. Small K^{eq} values ($K^{eq} \ll 1$) will have no effect on the diffusion in gels,

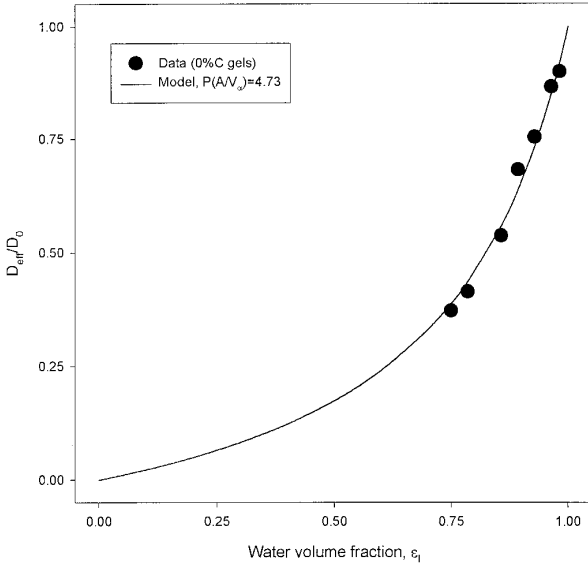


FIG. 9. The volume averaging model fit to the experimental diffusion data for polyacrylamide gels with no crosslinker.

which may explain the lack of crosslinker effect on the diffusion coefficients in gels.

From the volume averaging method, the diffusion coefficients for gels without the crosslinker are given by Eq. [21]. The term in large brackets on the right-hand side of Eq. [21] has been determined by Ryan (71) and represents the effect of geometrical structure on the effective diffusion coefficient. Figure 8 shows the effective diffusion coefficient determined by Eq. [21] as a function of porosity for several values of the term $P(A/V_\alpha)$. As shown in this figure, the effect of adsorption is to significantly reduce the effective diffusion coefficient, and this term has the potential to decrease the diffusion coefficient to a much larger degree than the term that accounts for the effect of geometry. By fitting Eq. [21] to the experimental data for gels with no crosslinker, the ratio $P(A/V_\alpha)$ was found to be 4.73. As shown in Fig. 9, the model (Eq. [43]) provided an excellent fit to the data. The value of $P(A/V_\alpha) = 4.73$ (error = 0.24%) will later be used in the analysis of the effective relaxivities.

The volume averaging theory can therefore describe the effects of a combination of factors, including adsorption and partitioning into the acrylamide fiber and the bisacrylamide crosslinker phases, on the diffusion coefficients in the gel.

Spin-Lattice Relaxation

Figure 10 shows a typical normalized magnetization recovery curve from the NMR data and the model given by Eq. [37]. The model provided an excellent fit to the data (corr = 0.99). The numerical values for k_{eff}^T were obtained using a nonlinear curve-fitting algorithm. The effective diffusion coefficients, D_{eff}^T , obtained from the NMR measurements, were substituted into Eq. [37] and the resulting equation was fit to the magnetization recovery experimental data to determine the effective relaxation coefficients.

The error in estimating k_{eff}^T was obtained by repeating the calculations for 2.5% T/5% C gels using experimental data from two consecutive runs on the same day, and data from a gel which had identical concentration, but was prepared at a different time. The resulting effective relaxation times, $1/k_{eff}^T = T_{eff}$, ranged from 3.022 to 3.161 s, with a relative percent error of 2%. The effective relaxation results were also checked for error due to diffusion. From the data reproducibility analysis, the diffusion coefficients for 20% T/5% C gels ranged from 1.36 to 1.461 (10^{-5} cm²/s). Upon substitution of these values (1.36 to 1.461 (10^{-5} cm²/s)) into the Eq. [37], the resulting effective relaxation time for this composition gel was unchanged, and found to equal 1.89 s. As a result, the experimental error in determining the diffusion coefficients has a negligible effect on the T_{eff} or k_{eff}^T values.

Figure 11 shows the relaxation time, $T_{1eff} = (k_{eff}^T)^{-1}$, as a function of the acrylamide concentration. The data is shown for gels with 0, 5, and 10% C concentration. As expected, the relaxation time, $(k_{eff}^T)^{-1}$, decreases as the concentration of the acrylamide increases. In order to compare the data to the models, the acrylamide concentration in Fig. 11 must be replaced with the volume fraction of water, ϵ_l . A commonly accepted value of 1.4 g/ml (79) was used as the density of acrylamide in a gel, and the volume fraction of water was calculated from $\epsilon_l = 1 - T/1.4$.

From the volume averaging method, at 0% crosslinker concentration, the effective relaxation rate constant, k_{eff}^T , is

$$k_{eff}^T \approx k_{eff}^\alpha = \frac{P(A/V_\alpha)k_f + \epsilon_l(k_l - P(A/V_\alpha)k_f)}{P(A/V_\alpha) + \epsilon_l(1 - P(A/V_\alpha))}. \quad [22]$$

Since the ratio $P(A/V_\alpha)$ was previously calculated as 4.73 from the diffusion data, and the bulk (free water) relaxation rate constant, k_l , was measured independently and found equal to 0.253 s^{-1} , the fiber surface relaxation rate constant, k_f , was

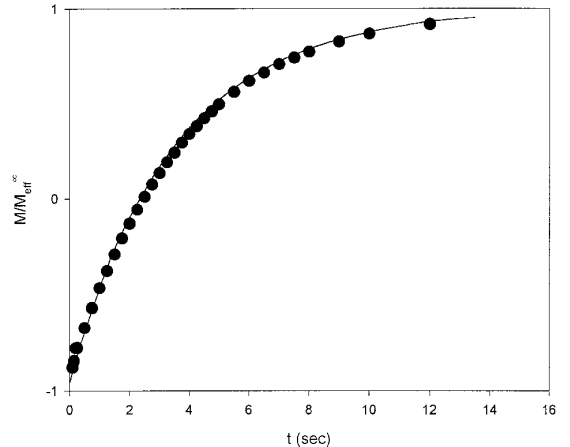


FIG. 10. A typical normalized magnetization recovery curve for polyacrylamide gels. Comparison to the spatial averaging model. ●, Data (2.5% T/0% C gel); —, model.

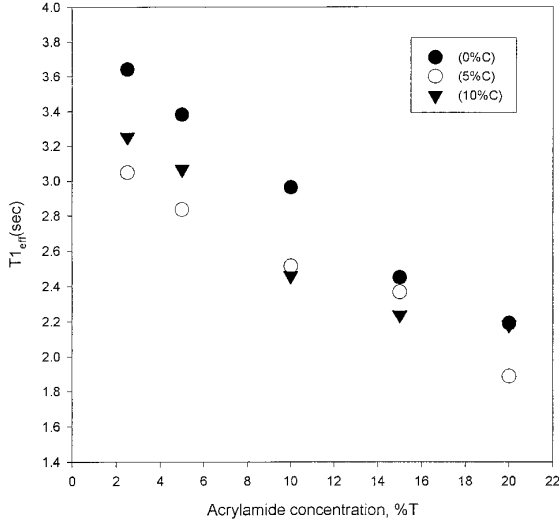


FIG. 11. Effective relaxation coefficient for polyacrylamide gels as a function of the total polymer concentration.

determined by fitting Eq. [22] to the experimental data. Figure 12 shows the model (Eq. [22]) with the best fit value $k_f = 0.668$ (error = 0.04%), and the experimental data for 0% crosslinked gels. As shown in Fig. 12, Eq. [22] fits the data very well.

For crosslinked gels, the expression for the effective relaxivities from the volume averaging model was

$$\begin{aligned}
 k_{eff}^T &= \frac{k_{eff}^\alpha \epsilon_\alpha + K^{eq} k_\beta \epsilon_\beta}{\epsilon_\alpha + K^{eq} \epsilon_\beta} \\
 &= \frac{1}{\epsilon_\alpha + K^{eq} \epsilon_\beta} \left[\left(\frac{P(A/V_\alpha) k_f + \epsilon_l (k_l - P(A/V_\alpha) k_f)}{P(A/V_\alpha) + \epsilon_l (1 - P(A/V_\alpha))} \right) \epsilon_\alpha \right. \\
 &\quad \left. + K^{eq} k_\beta \epsilon_\beta \right]. \quad [26]
 \end{aligned}$$

The volume fractions, ϵ_α and ϵ_β , can be expressed in terms of ϵ_f and ϵ_l , noting that $(\epsilon_\alpha + \epsilon_\beta) = 1$. Since the relative amount of the crosslinker (9×10^{-4} to 0.01 by volume fraction) is small, the fiber volume fraction, ϵ_f , can be based upon the concentration of acrylamide only. It is also assumed here, based upon the previous analysis of the diffusion data, that the equilibrium partition coefficient of protons between the crosslinker and the water phase, K^{eq} , is small ($K^{eq} \ll 1$). Equation [26] then reduces to

$$\begin{aligned}
 k_{eff}^T &= \left(\frac{P(A/V_\alpha) k_f + \epsilon_l (k_l - P(A/V_\alpha) k_f)}{P(A/V_\alpha) + \epsilon_l (1 - P(A/V_\alpha))} \right) \\
 &\quad + K^{eq} k_\beta \left(\frac{1 - \epsilon_l - \epsilon_f}{\epsilon_l + \epsilon_f} \right). \quad [44]
 \end{aligned}$$

Since the values $P(A/V_\alpha)$, k_f , and k_l are known, the product $K^{eq} k_\beta$ can now be obtained by fitting Eq. [44] to the experi-

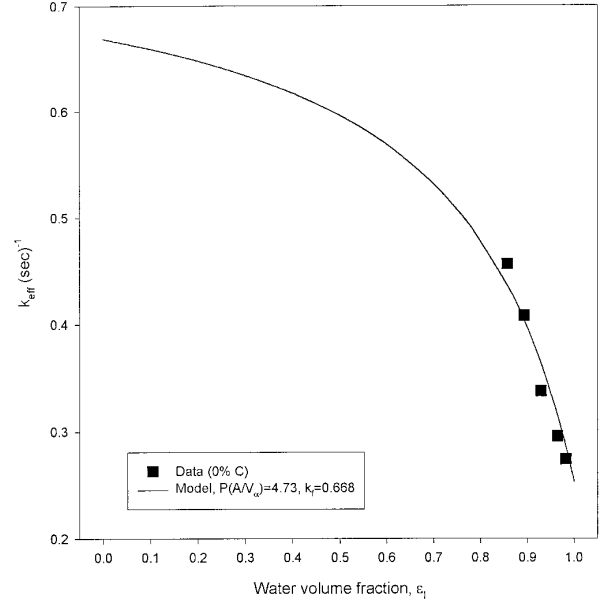


FIG. 12. The volume averaging model fit to the T_1 relaxation data for polyacrylamide gels with no crosslinker.

mental data. From the nonlinear regression analysis, the product $K^{eq} k_\beta$ was found to equal 10.3 s^{-1} (error = 2.83%) for 5% C gels, and 2.98 s^{-1} (error = 0.91%) for 10% C gels. Figure 13 shows the effective relaxation rate constant, k_{eff}^T data, and the model (Eq. [44]) using $K^{eq} k_\beta$ values of 10.3 and 2.98 s^{-1} for 5 and 10% gels, respectively, as functions of the inverse volume fraction, $(\epsilon_l + \epsilon_f)^{-1}$. The model, Eq. [44], provided an excellent fit to the data. As also shown in Fig. 13, the NMR

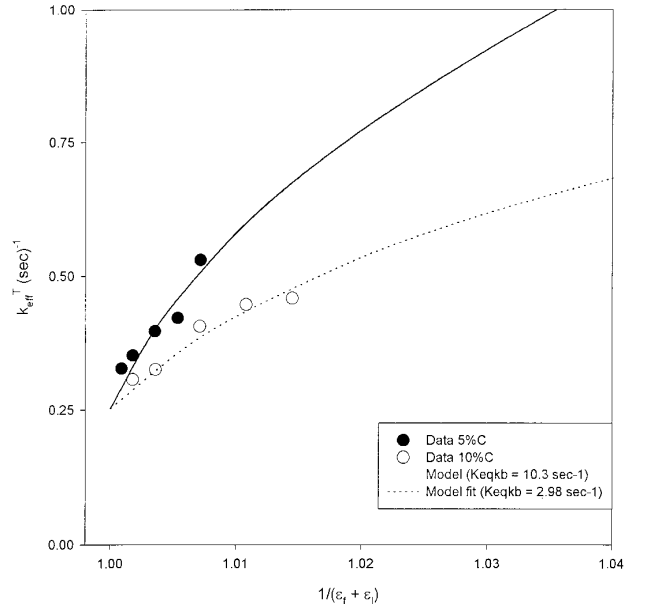


FIG. 13. The volume averaging model fit to the T_1 relaxation data for polyacrylamide gels with 5 and 10% crosslinker concentration.

relaxation data is very sensitive to small changes in the volume fraction, $(\epsilon_l + \epsilon_j)$. For a small increase in the inverse volume fraction, $(\epsilon_l + \epsilon_j)^{-1}$, from 1.00 to 1.02, the $K^{eq}k_\beta$ values more than tripled as the crosslinker concentration decreased from 5 to 10% C. Since the crosslinker, bisacrylamide, is water insoluble in the absence of acrylamide, the relaxation rate constants for the pure crosslinker phase cannot be determined experimentally. However, the crosslinker relaxation rate constant k_β is expected to be independent of gel composition since it is an intrinsic property of the Bis phase. This assumption, coupled with the preceding data, leads to the conclusion that as the concentration of the crosslinker is increased from 5 to 10% C, the equilibrium distribution coefficient, K^{eq} , decreases by a factor greater than 3. This is a clear indication that as the crosslinker concentration is raised, the Bis phase becomes increasingly hydrophobic.

DISCUSSION AND CONCLUSIONS

The degree of crosslinking is known to affect the size of the pores of polymer network, especially at high gel concentrations (80, 81). The effects of crosslinker on the structure of gels were previously investigated using light, small-angle neutron, and small-angle X-ray scattering (3, 5). All of the previous studies noted distinct structural changes with increasing crosslinker concentration. Although there is strong evidence that the structure of gels and particularly the pore size is affected by the concentration of the crosslinker, the present study demonstrates that the diffusion coefficients of water in gels are independent of the amount of crosslinker. The proposed explanation for this observation is that the equilibrium water partition coefficient between the bisacrylamide crosslinker phase and the bulk water phase, K^{eq} , is very small. As demonstrated using the Bloch equations and the volume averaging method, if K^{eq} is much less than 1, the crosslinker has no effect on the diffusion of water in gels. Furthermore, fitting the present experimental data to previously published diffusion models that account for fiber and solute size (18, 73, 39) required unrealistically low values for the acrylamide fiber size. Other models from the literature that account only for geometrical effects on diffusion predicted much higher diffusion coefficients than observed from the experimental results of the present study. The Mackie–Meares theory appeared to fit the experimental data adequately; however, this theory does not account for the crosslinker concentration, and it also is based on the unrealistic assumption that the acrylamide fiber is the same size as the solute. The volume averaging model developed in the present study incorporates the effects of adsorption to the surface of the uncrosslinked polyacrylamide fibers and to the bisacrylamide clusters on diffusion within one unified approach that also gives detailed expressions for the relaxation rate constants. This model demonstrates that the ratio PA/V_α may significantly lower the diffusion coefficients in gels.

Contrary to the diffusion data, T_1 relaxation measurements showed a detectable effect of crosslinker concentration on the relaxation of water in gels. The same mathematical model derived for the diffusion coefficients using the Bloch equations and the volume averaging method (45, 46) could also be used to describe the effects of adsorption and gel structure on the magnetization recovery. The proposed model for the gel medium consisted of a three-phase system including the bulk water, the uncrosslinked acrylamide fibers, and the crosslinker phases. This model follows the cluster concept introduced by Richards and Temple (26). The effects of the crosslinker concentration were accounted for by introducing the proton partition coefficient, K^{eq} , between the crosslinker and bulk water phases. In addition, the effects of adsorption to the surface of the fibers were also incorporated in the model. By fitting the model to the experimental data, the product $K^{eq}k_\beta$ for 5% C gels was found to be larger than that for 10% C gels. Since k_β is a constant, it can be concluded that increasing the crosslinker concentration from 5 to 10% C causes a more than threefold decrease in the equilibrium coefficient K^{eq} . The resulting reduction in the value of K^{eq} implies that at high concentrations of crosslinker, water protons are less likely to penetrate the crosslinker region. This observation is in general agreement with the cluster concept introduced by Richards and Temple (26) and previously published experimental data by Cohen *et al.* (3). Since the crosslinker is known to be more hydrophobic than acrylamide, at high concentrations it will form hydrophobic clusters. The use of the Bloch equations provided an accurate description of the proton relaxation in the hydrogels. The derived relaxation equations were successful in describing the general trends seen from the experimental data.

The T_1 relaxation analysis presented in this study differs significantly from previously published methods for examining the structural features of the gels using spin–lattice relaxation. One previous approach used a diffusion cell model, strictly valid for media with micrometer-sized pores, to analyze relaxation in polyacrylamide gels where the pores are only a few nanometers in length (11). In this previous study (11), a pore size distribution on the nanometer length scale was calculated for the polyacrylamide gel. It is, however, not clear that this distribution is physically meaningful, since the time scales for the experimental measurements were too long to adequately describe features of the gel on the nanometer length scale. The present study, in contrast, describes how, with the use of the averaging approach, the structure of polyacrylamide gels can be analyzed using proton T_1 relaxation data in combination with water self-diffusion measurements.

ACKNOWLEDGMENTS

We are grateful to Ms. Lori McFadden for gel preparation, and Mr. Dick Rosanske and Dr. Thomas Gadris for assistance with NMR relaxation measurements. We would also like to acknowledge the National High Magnetic Field Laboratory and the Department of Chemistry at Florida State University for use of NMR instrumentation. This work was supported by a grant (UGS95-0041) from the National Aeronautics and Space Administration.

REFERENCES

1. J. G. H. Joosten, J. L. McCarthy, and P. N. Pusey, Dynamic and static light scattering by aqueous polyacrylamide gels, *Macromolecules* **24**, 6690–6699 (1991).
2. L. Fang, W. Brown, and C. Konak, Dynamic properties of polyacrylamide gels and solutions, *Polymer* **31**, 1960–1967 (1990).
3. Y. Cohen, O. Ramon, I. J. Kopelman, and S. Mizrahi, Characterization of inhomogeneous polyacrylamide hydrogels, *J. Polym. Sci. B: Polym. Phys.* **30**, 1055–1067 (1992).
4. D. B. Sellen, Laser light scattering study of polyacrylamide gels, *J. Polym. Sci. B: Polym. Phys.* **25**, 699–716 (1987).
5. A.-M. Hecht, R. Duplessix, and E. Geissler, Structural inhomogeneities in the range 2.5–2000 angstroms in polyacrylamide gels, *Macromolecules* **18**, 2167–2173 (1985).
6. S. Mallam, F. Horkay, A.-M. Hecht, and E. Geissler, Scattering and swelling properties of inhomogeneous polyacrylamide gels, *Macromolecules* **22**, 3356–3361 (1989).
7. J. P. Baker, L. H. Hong, H. W. Blanch, and J. M. Prausnitz, Effect of initial total monomer concentration on the swelling behavior of cationic acrylamide-based hydrogels, *Macromolecules* **27**, 1446–1454 (1994).
8. N. Weiss, T. van Vliet, and A. Silberberg, Permeability of heterogeneous gels, *J. Polym. Sci.* **17**, 2229–2240 (1979).
9. A. Suzuki, A. M. Yamazaki, and Y. Kobiki, Direct observation of polymer gel surfaces by atomic force microscopy, *J. Chem. Phys.* **104**, 1751–1757 (1996).
10. G.-L. Ding, L. Y. Li, Y.-R. Du, and C.-H. Ye, NMR microscopy of polyacrylamide hydrogel, *Magn. Reson. Imaging* **14**, 947–948 (1996).
11. M. Chui, R. Phillips, and M. McCarthy, Measurement of the porous microstructure of hydrogels by nuclear magnetic resonance, *J. Colloid Interface Sci.* **174**, 336–344 (1995).
12. R. P. Kennan, K. A. Richardson, J. Zhong, M. J. Maryanski, and J. C. Gore, The effects of cross-link density and chemical exchange on magnetization transfer in polyacrylamide gels, *J. Magn. Reson. B* **110**, 267–277 (1996).
13. J. P. Cohen-Addad, NMR and fractal properties of polymeric liquids and gels, *Prog. NMR Spectrosc.* **25**, 1–316 (1993).
14. J. P. Cohen-Addad, NMR and statistical structures of gels, in "The Physical Properties of Polymeric Gels" (J. P. Cohen Addad, Ed.), pp. 39–86. Wiley, Chichester (1996).
15. C. Morrison and R. M. Henkelman, A model for magnetization transfer in tissue, *Magn. Reson. Medicine* **33**, 475–482 (1995).
16. R. M. Henkelman, G. J. Stanisz, J. K. Kim, and M. J. Bronskill, Anisotropy of NMR properties of tissues, *Magn. Reson. Medicine* **32**, 592–601 (1994).
17. R. Harrison, M. J. Bronskill, and R. M. Henkelman, Magnetization transfer and T2 relaxation components in tissue, *Magn. Reson. Medicine* **33**, 490–496 (1995).
18. A. G. Ogston, The spaces in a uniform random suspension of fibres, *Trans. Faraday Soc.* **54**, 1754–1757 (1958).
19. D. Rodbard and A. Chrambach, Unified theory of gel electrophoresis and gel filtration, *Proc. Natl. Acad. Sci. USA* **65**, 970–977 (1970).
20. A. Chrambach and D. Rodbard, Polyacrylamide gel electrophoresis, *Science* **172**, 440–451 (1971).
21. D. Rodbard and A. Chrambach, Estimation of molecular radius, free mobility, and valence using polyacrylamide gel electrophoresis, *Anal. Biochem.* **40**, 95–134 (1971).
22. D. Rodbard, Estimation of molecular weight by gel filtration and gel electrophoresis I. Mathematical principles, in "Methods of Protein Separation" (N. Catsimpoilas, Ed.), pp. 145–179. Plenum, New York (1976).
23. D. Rodbard, Estimation of molecular weight by gel filtration and gel electrophoresis II. Statistical and computational considerations, in "Methods of Protein Separation" (N. Catsimpoilas, Ed.), pp. 181–207. Plenum, New York (1976).
24. P. G. Righetti, On the pore size and shape of hydrophilic gels for electrophoretic analysis, in "Electrophoresis '81," pp. 3–16. de Gruyter, Berlin (1981).
25. J. C. Giddings, E. Kucera, C. P. Russell, and M. N. Myers, Statistical theory for the equilibrium distribution of rigid molecules in inert porous networks, exclusion chromatography, *J. Phys. Chem.* **72**, 4397–4408 (1968).
26. E. G. Richards and C. J. Temple, Some properties of polyacrylamide gels, *Nature* **230**, 92–96 (1971).
27. J. S. Fawcett and C. J. O. R. Morris, Molecular-sieve chromatography of proteins on granulated polyacrylamide gels, *Sep. Sci. Technol.* **1**, 9–26 (1966).
28. C. J. O. R. Morris and P. Morris, Molecular-sieve chromatography and electrophoresis in polyacrylamide gels, *Biochem. J.* **124**, 517–528 (1971).
29. D. Rodbard and A. Chrambach, in "Electrophoresis and Isoelectric Focusing in Polyacrylamide Gels" (R. C. Allen and H. R. Mauer, Eds.), p. 28, de Gruyter, New York (1974).
30. M. L. White and G. H. Dorion, Diffusion in a crosslinked acrylamide polymer gel, *J. Polym. Sci.* **55**, 731–740 (1961).
31. Y. Suzuki and I. Nishio, Quasielastic-light-scattering study of the movement of particles in gels: topological structure of pores in gels, *Phys. Rev. B* **45**, 4614–4619 (1992).
32. I. Nishio, J. C. Reina, and R. Bansil, Quasielastic light-scattering study of the movement of particles in gels, *Phys. Rev. Lett.* **59**, 684–687 (1987).
33. J. G. H. Joosten, and E. T. F. Gelade, Dynamic light scattering by nonergodic media: Brownian particles trapped in polyacrylamide gels, *Phys. Rev. A* **42**, 2161–2175 (1990).
34. L. Pavesi and A. Rigamonti, Diffusion constants in polyacrylamide gels, *Phys. Rev. E* **51**, 3318–3323 (1995).
35. B. Balcom, A. Fischer, T. Carpenter, and L. Hall, Diffusion in aqueous gels. Mutual diffusion coefficients measured by one-dimensional nuclear magnetic resonance imaging, *J. Am. Chem. Soc.* **115**, 3300–3305 (1993).
36. S. J. Gibbs and C. S. Johnson, Pulsed field gradient NMR study of probe motion in polyacrylamide gels, *Macromolecules* **24**, 6110–6113 (1991).
37. S. J. Gibbs, A. S. Chu, E. N. Lightfoot, and T. W. Root, Ovalbumin diffusion at low ionic strength, *J. Phys. Chem.* **95**, 467–471 (1991).
38. W. Brown and R. M. Johnsen, Diffusion in polyacrylamide gels, *Polymer* **22**, 185–189 (1981).
39. C. J. O. R. Morris, Gel filtration and gel electrophoresis, in "Protides of the Biological Fluids" (H. Peeters, Ed.), Vol. 14, pp. 543–551. Elsevier, Amsterdam (1966).
40. W. M. Deen, Hindered transport of large molecules in liquid-filled pores, *AIChE J.* **33**, 1409–1425 (1987).
41. R. J. Phillips, W. M. Deen, and J. F. Brady, Hindered transport in fibrous membranes and gels: Effect of solute size and fiber configuration, *J. Colloid Interface Sci.* **139**, 363–373 (1990).
42. L. Johansson and J.-E. Lofroth, Diffusion and interaction in gels

- and solutions. 4. Hard sphere Brownian dynamics simulations, *J. Chem. Phys.* **98**, 7471–7479 (1993).
43. L. Johansson and C. Elvingson, Diffusion and interaction in gels and solutions. 3. Theoretical results on the obstruction effect, *Macromolecules* **24**, 6024–6029 (1991).
 44. L. Johansson, U. Skantze, and J.-E. Lofroth, Diffusion and interaction in gels and solutions. 2. Experimental results on the obstruction effect, *Macromolecules* **24**, 6019–6023 (1991).
 45. S. Whitaker, Diffusion and dispersion in porous media, *AIChE J.* **13**, 420–427 (1967).
 46. R. G. Carbonell and S. Whitaker, Heat and mass transfer in porous media, in "Fundamentals of Transport Phenomena in Porous Media" (J. Bear and M. Y. Corapciolu, Eds.), pp. 121–200. Nijhoff, Dordrecht (1984).
 47. S. Whitaker, Transient diffusion, adsorption and reaction in porous catalysts: The reaction controlled, quasi-steady catalytic surface, *Chem. Engr. Sci.* **41**, 3015–3022 (1986).
 48. S. Whitaker, The species mass jump condition at a singular surface, *Chem. Engr. Sci.* **47**, 1677–1685 (1992).
 49. J. A. Ochoa, "Diffusion and Reaction in Heterogeneous Media," Ph.D. Dissertation, University of California, Davis, p. 475 (1988).
 50. D. J. Ryan, R. G. Carbonell, and S. Whitaker, A theory of diffusion and reaction in porous media, *AIChE Symp. Ser.* **71**, 46–62 (1981).
 51. M. Quintard and S. Whitaker, Transport in ordered and disordered porous media: Volume-averaged equations, closure problems, and comparison with experiment, *Chem. Engr. Sci.* **14**, 2537–2564 (1993).
 52. F. Bloch, Nuclear induction, *Phys. Rev.* **70**, 460 (1946).
 53. M. H. Cohen and K. S. Mendelson, Nuclear magnetic relaxation and the internal geometry of sedimentary rocks, *J. Appl. Phys.* **53**, 1127–1135 (1982).
 54. K. S. Mendelson, Nuclear magnetic resonance in sedimentary rocks: Effect of proton desorption rate, *J. Appl. Phys.* **53**, 6465–6466 (1982).
 55. K. S. Mendelson, Nuclear magnetic relaxation in fractal pores, *Phys. Rev. B* **34**, 6503–6505 (1986).
 56. D. Wu, A. Chen, and C. S. Johnson, An improved diffusion-ordered spectroscopy experiment incorporating bipolar-gradient pulses, *J. Magn. Reson. A* **115**, 260–264 (1995).
 57. S. J. Gibbs and C. S. Johnson, A PFG NMR experiment for accurate diffusion and flow studies in the presence of eddy currents, *J. Magn. Reson.* **93**, 395 (1991).
 58. J. E. Tanner, Use of stimulated echo in NMR diffusion studies, *J. Chem. Phys.* **52**, 2523 (1970).
 59. E. O. Stejskal and J. E. Tanner, Spin diffusion measurement: Spin echoes in the presence of a time-dependent field gradient, *J. Chem. Phys.* **42**, 288 (1965).
 60. I. Nozad, R. G. Carbonell, and S. Whitaker, Heat conduction in multiphase systems—I. Theory and experiment for two-phase systems, *Chem. Engr. Sci.* **40**, 843–855 (1985).
 61. J. H. Kim, J. A. Ochoa, and S. Whitaker, Diffusion in anisotropic porous media, *Transp. Porous Media* **2**, 327–356 (1987).
 62. J. A. Ochoa-Tapia, P. Stroeve, and S. Whitaker, Diffusive transport in two-phase media: Spatially periodic models and Maxwell's theory for isotropic and anisotropic systems, *Chem. Engr. Sci.* **49**, 709–726 (1994).
 63. J. A. Ochoa-Tapia, P. Stroeve, and S. Whitaker, Diffusion and reaction in cellular media, *Chem. Engr. Sci.* **41**, 2999–3013 (1986).
 64. A. G. Ogston, B. N. Preston, and J. D. Wells, On the transport of compact particles through solutions of chain-polymers, *Proc. R. Soc. Lond. A* **333**, 297–316 (1973).
 65. A. T. Andrews, "Electrophoresis," 2nd ed. Clarendon, Oxford (1986).
 66. T. B. Anderson and R. Jackson, A fluid mechanical description of fluidized beds, *Ind. Eng. Chem. Fundam.* **6**, 527–539 (1967).
 67. S. Whitaker, Simultaneous heat, mass, and momentum transfer in porous media: A theory of drying, *Advan. Heat Transfer III* **13**, 119 (1977).
 68. B. Penke, "Analysis of Diffusion and Structure in Polyacrylamide Gels by Nuclear Magnetic Resonance," M.S. Thesis, Florida State University (1997).
 69. J. C. Maxwell, "Electricity and Magnetism," 2nd ed., pp. 435–445. Clarendon, Oxford (1892).
 70. W. T. Perrins, D. R. McKenzie, and R. C. McPhedran, Transport properties of regular arrays of cylinders, *Proc. R. Soc. Lond. A* **369**, 207–225 (1979).
 71. D. J. Ryan, "Effective Diffusivities in Reactive Porous Media," M.S. Thesis, Department of Chemical Engineering, University of California, Davis, California (1983).
 72. N. Wakao and J. M. Smith, Diffusion in catalyst pellets, *Chem. Eng. Sci.* **17**, 825–834 (1962).
 73. J. S. Mackie and P. Meares, The diffusion of electrolytes in a cation-exchange resin membrane I. Theoretical, *Proc. R. Soc. Lond. A* **232**, 498–509 (1955).
 74. A. Einstein, On the movement of small particles suspended in stationary liquids required by molecular-kinetic theory of heat, *Annalen Physik* **17**, 549 (1905).
 75. H. J. V. Tyrell and K. R. Harris, "Diffusion in Liquids," p. 331. Butterworth, Stoneham, MA (1984).
 76. J. Tong and J. L. Anderson, Partitioning and diffusion of proteins and linear polymers in polyacrylamide gels, *Biophys. J.* **70**, 1505–1513 (1996).
 77. G. W. Jackson and D. F. James, The permeability of fibrous porous media, *Can. J. Chem. Eng.* **64**, 364–374 (1986).
 78. M. Tokita, T. Miyoshi, K. Takegoshi, and K. Hikichi, Probe diffusion in gels, *Phys. Rev. E* **53**, 1823–1827 (1996).
 79. P. Munk, T. M. Aminabhavi, P. Williams, and D. E. Hoffman, Some solution properties of polyacrylamide, *Macromolecules* **13**, 871–875 (1980).
 80. J. Margolis and C. W. Wrigley, Improvement of pore gradient electrophoresis by increasing the degree of cross-linking at high acrylamide concentrations, *J. Chromatogr.* **106**, 204–209 (1975).
 81. D. Asnaghi, M. Giglio, A. Bossi, and P. G. Righetti, Quasi-ordered structure in highly crosslinked poly(acrylamide) gels, *Macromolecules* **30**, 6194–6198 (1997).